

# Non-unital noise in a superconducting quantum computer as a computational resource for reservoir computing

Francesco Monzani, Emanuele Ricci, Luca Nigro, and Enrico Prati\*

*Dipartimento di Fisica "Aldo Pontremoli", Università degli Studi di Milano, Via Celoria 16, 20133, Milan, Italy*

Despite theoretical promises, most machine learning algorithms fail on current quantum computers due to overwhelming noise. Nevertheless, many recurrent architectures are most efficient if they can process information by progressively reducing the correlation on inputs from earlier time steps. Among them, reservoir computing represents a major paradigm of artificial intelligence for processing time-dependent tasks thanks to the involvement of fading memory. Despite attempts to demonstrate quantum reservoir computing based on intentional perturbations of the network, whether the intrinsic noise of the quantum circuit can be straightforwardly exploited remained unknown. We show the feasibility of reservoir computing on a circuit of superconducting qubits based on the unavoidable dissipation typical of NISQ devices. We prove that noise modeled by a non-unital quantum channel ensures the functioning of a quantum echo state network. In particular, amplitude damping is responsible for drastically improving the short-term memory capacity and expressivity of the network, by simultaneously providing fading memory and richer dynamics. Our experimental results pave the way for the application of reservoir computing methods in non-fault-tolerant quantum computers.

## INTRODUCTION

The intrinsic dissipation and decoherence in noisy intermediate-scale quantum (NISQ) computers pose a major limitation in many machine-learning protocols [1], restricting the natural application of quantum computing in artificial intelligence [2, 3]. Nevertheless, dissipation may serve as a fully-fledged resource for quantum computation [4–6]. Our results show that the action of specific quantum noise in the hardware, namely noise modeled by non-unital quantum channels, significantly improves the short-term memory capacity and expressivity of a quantum network, proving the reliability of quantum reservoir computing as a valid computational architecture for memory-dependent tasks employing a gate-based quantum computer. We emphasize that an in-depth study of the beneficial computational effects of non-unital noise in quantum machine learning is only in its early stages [7], unveiling, for example, a promising application in avoiding barren plateaus in variational problems [8]. Reservoir computing is a well-established supervised machine learning algorithm that employs a fixed neural network – the reservoir, to process time-dependent information. In addition to initial digital and neuromorphic proposals, respectively, the echo state network [9] and the liquid state machine [10], reservoir computing has proven effective in a wide range of unconventional deployments [11]. Among several physical implementations [12], the exponentially large computational capacity of quantum systems has been harnessed for reservoir computing [13, 14], employing photonic circuits [15–17], bosonic oscillators [18, 19], fermionic systems [20, 21], neutral atoms [22] and spin networks [23–28]. Focusing on superconducting quantum computers, we refer to Ref. [29, 30] for early implementations, more recently empowered by mid-circuit measurements [31]. Reservoir computing appears particularly

suitable for leveraging quantum computing, as it does not require any training in the parameters of the quantum evolution. An essential feature essential for reservoir computing is the so-called fading memory [32, 33]. Namely, a reservoir network is most efficient if the information is processed by progressively reducing the emphasis on inputs from earlier time steps. Dissipation has recently been recognized as a powerful computational resource in reservoir architectures that employ spin dynamics [27]. In contrast, phase errors seem to have no utility for quantum computing, since they are theoretically associated with loss of quantum information. Concerning reservoir computing employing superconducting quantum computers, artificial manual reset of the information flow has proven to be a reliable resource for fading memory in memory-dependent tasks [30, 34]. Here, we step further by demonstrating how the intrinsic noise in superconducting quantum computers can be harnessed to spontaneously ensure the functioning of a quantum echo state network. We implement reservoir computing on a circuit of 7 superconducting qubits and we perform its emulation by including a realistic noise model. By testing our quantum echo state network on standard memory-dependent benchmarks, we recognize which type of noise benefits the performances. Thus, we show that noise modeled by a non-unital channel is needed to simultaneously guarantee memory capacity and accuracy in nonlinear time-dependent tasks. This confirms early results for memory-independent classification tasks [35]. We recall that a quantum channel is unital if it preserves the identity in the operator space. Remarkably, the quantum channel modeling the noise of a superconducting quantum computer falls within such a class of non-unital noise. As typically observed in recurrent networks [36, 37], we identify a critical regime tuned by noise intensity, in which several network capabilities, such as

short-term memory capacity and expressivity, are maximized. In this respect, we suitably slowed the execution of the circuit accordingly to maximize the learning accuracy. Finally, the universality of a neural network architecture is responsible for its computational effectiveness, since it ensures that any input-output mapping can be approximated with arbitrary precision [10, 18, 27, 29, 38–40]. Here, we provide strong theoretical support to our empirical findings, by proving the universality of our gate-based echo state network under the effect of non-unital quantum channels. Our experiment paves the way for real-world application of quantum reservoir computing on noisy intermediate-scale and early fault-tolerant quantum computers.

## RESULTS

In order to demonstrate the feasibility of quantum reservoir computing on a noisy gate-based quantum computer, we proceed by first defining the embodiment of reservoir computing over the qubits. Next, we emulate the response of the reservoir by involving different kinds of noise to confirm that – as predicted, only the non-unital noise guarantees non-trivial dynamics required for the learning. According to realistic noise models, being non-unital noise a relevant component in that of superconducting quantum computers, we, therefore, move to such hardware implementation to demonstrate experimentally the learning. As the amount of noise determines the accuracy of the learning, the experiment takes into account a tuning of the execution time in order to maximize the accuracy.

### Problem setting

The task consists of defining a mapping – usually called *filter*, in the framework of reservoir computing, sending an input time series  $u \in \mathcal{I}$  into another target time series  $y \in \mathcal{O}$ , through read-out operations of the information encoded in the reservoir. The schematic structure is represented in Fig. 1. Denoting  $\mathcal{S}(\mathcal{H})$  the set of density operators  $\rho(t)$  on the Hilbert space  $\mathcal{H}$  that describes some quantum system, a quantum reservoir computer is described by the equations

$$\begin{cases} \rho_{t+1} = \mathcal{T}(\rho_t, u_{t+1}) \\ y_{t+1} = h(\rho_{t+1}) \end{cases} \quad (1)$$

expressing the time evolution of the density matrix over discretized time intervals denoted as  $\dots \rho_{t-1}, \rho_t, \rho_{t+1} \dots$ . Here,  $\mathcal{T} : \mathcal{S}(\mathcal{H}) \rightarrow \mathcal{S}(\mathcal{H})$  is any quantum channel that describes the dynamics of the quantum system and  $h$  is a suitable readout operation. The reservoir computer defines the filter, consisting of a unique and causal operator,

$\mathcal{C} : \mathcal{I} \rightarrow \mathcal{O}$  defined by the mapping

$$y_t = \mathcal{C}(u)_t = \mathcal{C}(u_{|_t}) = h(\mathcal{T}(\rho_{t-1}, u_t)) \quad (2)$$

where  $u_{|_t} = (u_0, \dots, u_{t-1}, u_t)$  indicate the input sequence truncated at time  $t$ . In this work, we employ a gate-based quantum echo state network [41] to process time-dependent information. We rely on the logical embodiment of the node of the reservoir by the  $4^N - 1$ , where  $N$  is the number of qubits, basis elements expressed by the Pauli operators  $(I, \sigma_x, \sigma_y, \sigma_z)$  as from the implementation introduced by Ref. [23]. In this framework, the output nodes correspond to the readout of single qubits  $\dots I \otimes \sigma_{z(i)} \otimes I, \dots$ . Its architecture is described in detail in the Methods. We test our computational machine by reproducing nonlinear, time-dependent mappings  $S(u) = \hat{y}$  between two time-dependent real sequences  $u = \{u_t\}_{t=0, \dots, L}$  and  $\hat{y} = \{\hat{y}_t\}_{t=0, \dots, L}$ . Specifically, we train the reservoir computer to minimize the distance

$$\text{dist}(\mathcal{C}(u), S(u)). \quad (3)$$

The tasks are selected among well-established benchmarks in the literature of reservoir computing, more specifically we consider NARMA tasks, up to  $n = 8$ , as described in the Methods. Both the emulator of the IBM-Osaka and the real quantum computer IBM-Brisbane have been exploited to perform the learning tasks. For what concerns the simulation of diverse models of quantum noise, their effect on the learning capabilities of the network is investigated by systematically tuning its intensity in numerical experiments. Throughout the whole Results section, the parameter that tunes noise intensity is referred to with  $\gamma$ .

### Impact of noise on the fading memory

The action of noise provides fading memory to the system by gradually reducing the network's dependence on past inputs. Indeed, the action of the quantum channel sequentially modifies the state of each qubit, contributing to the loss of information over time. We remark that fading memory is essential in reservoir computing, as it enables the network to integrate online new information. To assess how increasing noise affects the network's dependence on past inputs, we analyze its impact on the correlation between consecutive qubit measurements. See Methods for a detailed description of the architecture of our echo state network. After repeating the execution for  $S \sim 10^5$  shots, to reconstruct the average value of the  $\sigma_{Z(i)}$  Pauli observables, we compute, for any measured qubit,

$$\text{corr}(\bar{z}_t^i, \bar{z}_{t-k}^i), \quad (4)$$

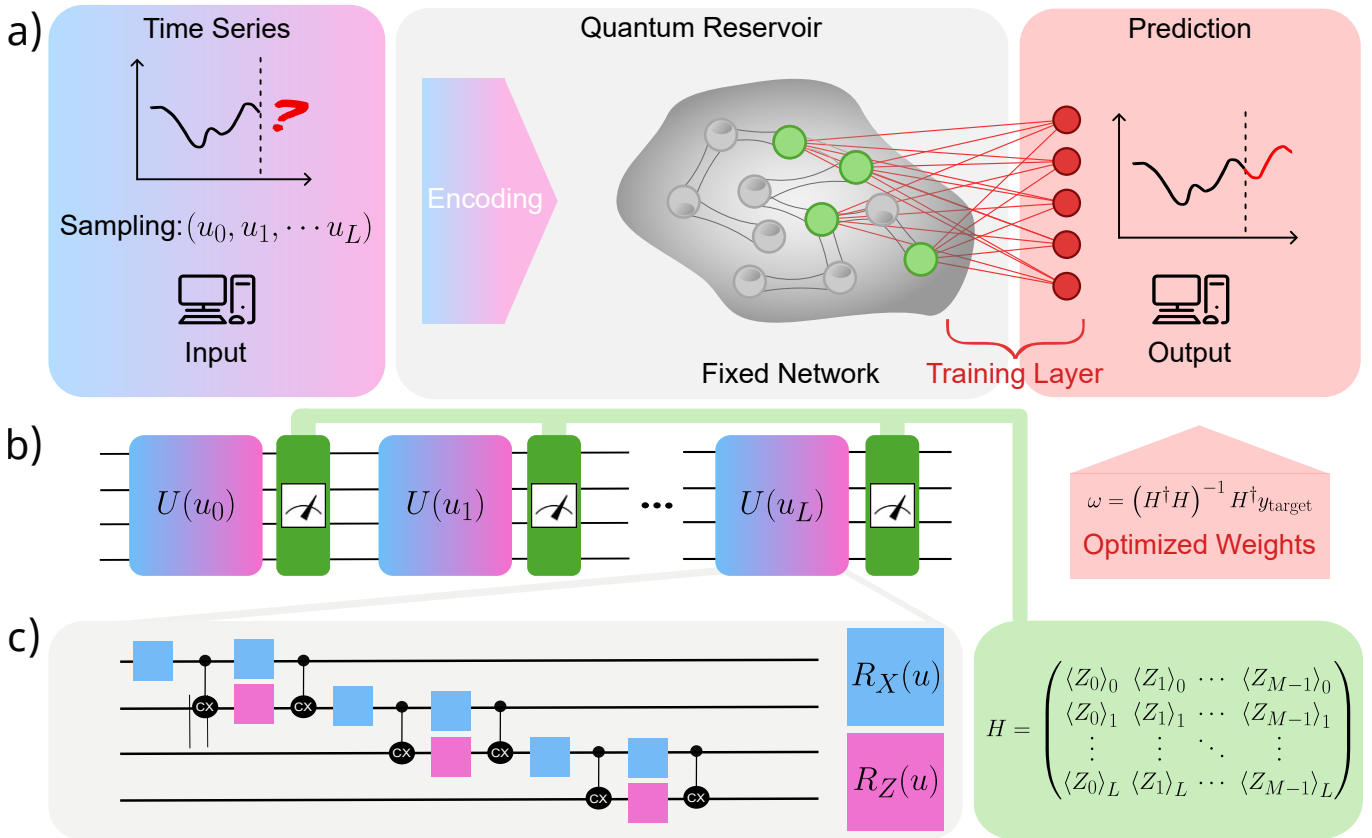


FIG. 1. **The architecture of quantum reservoir computing.** a) The time-dependent information in the input is sampled to produce the input time series. The information is stored in the logical nodes described by the Pauli basis associated with the qubits. During the evolution of the reservoir, the information is extracted by mid-circuit measurements of the true nodes (in green) of the network. The reservoir signal is the outcome of the measurements. The only trained part of the system is the readout weights  $\omega$  (red connections). b) The circuit is employed as the reservoir of the quantum echo state network. The input values are encoded in parametric unitary gates. Mid-circuit measurements are performed, to extract the reservoir signal online. After the execution, the optimal weights of the linear readout are computed through the pseudoinverse of the overall reservoir signal along the training interval, in order to minimize the distance from the target time series. c) The precise architecture of the gates in each unitary layer. The inputs are encoded in the composition of rotations along the  $X$  (in blue) and  $Z$  (in pink) axis of the Bloch sphere.  $Z$  Pauli operators are measured as true nodes. CNOT operators allow for the entanglement of the qubits. The qubits are left in the collapsed state after each measurement. In the work, we fix  $N = 7$  as the number of qubits. Finally, the reservoir signal, namely the expected value of each  $Z$  operator, is collected in the matrix  $H$ .

where the vector  $\vec{z}_t^i = \{(z_t)_s\}_{s=1, \dots, S}$  contains the outcomes of measurements for each repetition of the experiment. Then, we compute the mean correlation over the whole execution by averaging over  $t$ . Fig. 2 shows the mean correlation over time for increasing time windows  $k$ . As expected, higher noise intensity enhances the progressive loss of correlation. The loss of correlation appears comparable for different noise models. Thus, fading memory alone does not a priori justify the beneficial effect of amplitude damping on the short-term memory capacity of the network and its accuracy in learning tasks. From a theoretical point of view, fading memory is related to the contractivity of the evolution of the echo state network [39]. In our model, the contractivity in trace norm is ensured by the action of noise, as discussed in the Supplementary Material.

### Effect on learning of different simulated quantum noise models

After confirming that any contractive noisy channel ensures the fading memory of the network, we investigate their beneficial effect on the predictive capabilities of the architecture using two standard benchmarks for recurrent networks, namely the measure of short-term memory capacity (MC) and the non-linear autoregressive moving average (NARMA) task, presented in detail in Subsection "Benchmark for performance analysis". The short-term memory capacity measures the ability of the network to reproduce online a delayed window of the time-dependent input, while the NARMA task requires approximating a non-linear functional that depends on a fixed amount of the recent information in the input

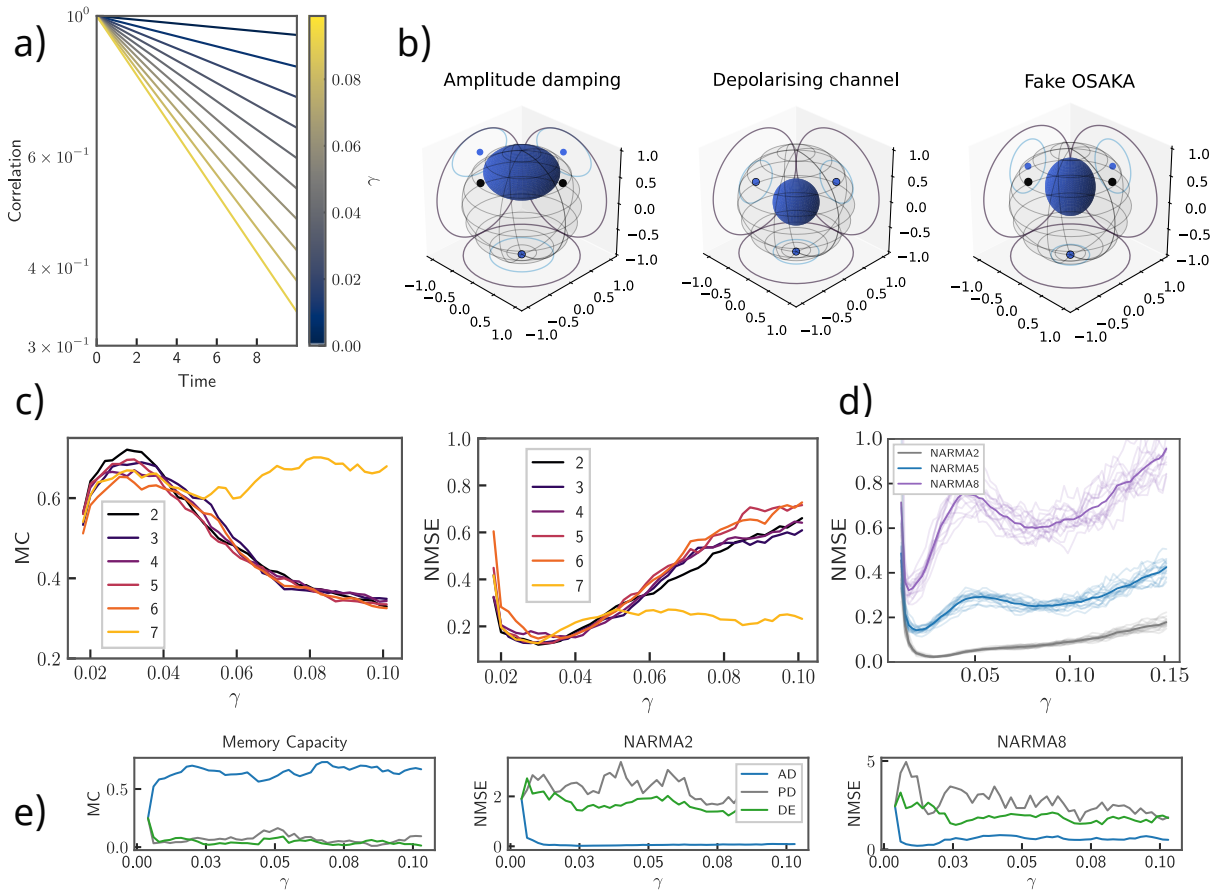


FIG. 2. **Effect on different noises on learning.** a) Decay over time in the mean correlation in subsequent measurements is enhanced by increasing amplitude damping intensity. Yellow lines indicate a higher intensity of the noise. The thickness of lines is proportional to the accuracy in NARMA5 prediction. b) From left to right, the blue area is the image of the quantum channel on the Bloch sphere. Black and blue dots are the projection of the sphere's center, respectively, before and after the application of the channel. For clarity, simulations are for  $\gamma = 0.6$  and tenfold intensity of noise in the IBM\_OSAKA backend. c) Accuracy in NARMA task and short-term memory capacity for a different number of measured qubits in the 7 qubits register. Yellow lines correspond to complete measurements. Running average on a window of ten values of  $\gamma$  is performed for smoother visualization. d) Accuracy in NARMA tasks with complete measurement of the register under the effect of increasing amplitude damping. Results for a swarm of 20 executions are plotted in transparency, mean values are in bold in the picture. Running average on a window of ten values of  $\gamma$  is performed for smoother visualization. The optimal noise regime corresponds to  $\gamma \sim 0.03$ . e) Accuracy in reproducing NARMA tasks and memory capacity for increasing intensity of amplitude damping (in blue), phase damping (in grey), and depolarizing channel (in green). Only amplitude damping ensures the learning of the network.

time series. Three noise models are applied separately, namely amplitude damping, phase damping, and depolarizing. Among them, only the amplitude damping is non-unital. Remarkably, we observe that the action of the only amplitude damping drastically enhances the memory capacity of the network. Consistently, the higher memory capacity is reflected in better accuracy in reproducing the time-dependent task. On the other hand, phase damping and depolarizing noise have detrimental effects on both memory capacity and accuracy. These results are summarized in Fig. 2, showing the normalized mean square error (NMSE) and MC for increasing the intensity of the three noises considered. The beneficial effect of amplitude damping is justified by its non-

unital nature as a quantum channel. Indeed, the action of a non-unital channel enriches the dynamics of the reservoir allowing for a wider exploration of the phase space and, consequently, greater storage of information. We discuss more details about non-unital channels and theoretical insight into the role of unitality in quantum reservoir computing in the Supplementary Material. To anticipate the behavior on NISQ hardware, we repeated the experiment by applying a channel that replicates the noise model of the backends provided by IBM. A realistic noise model for current superconducting hardware consists of the application of the composition of quantum channels, including, but not restricted to, the three noise models considered in this work. Thus, recalling

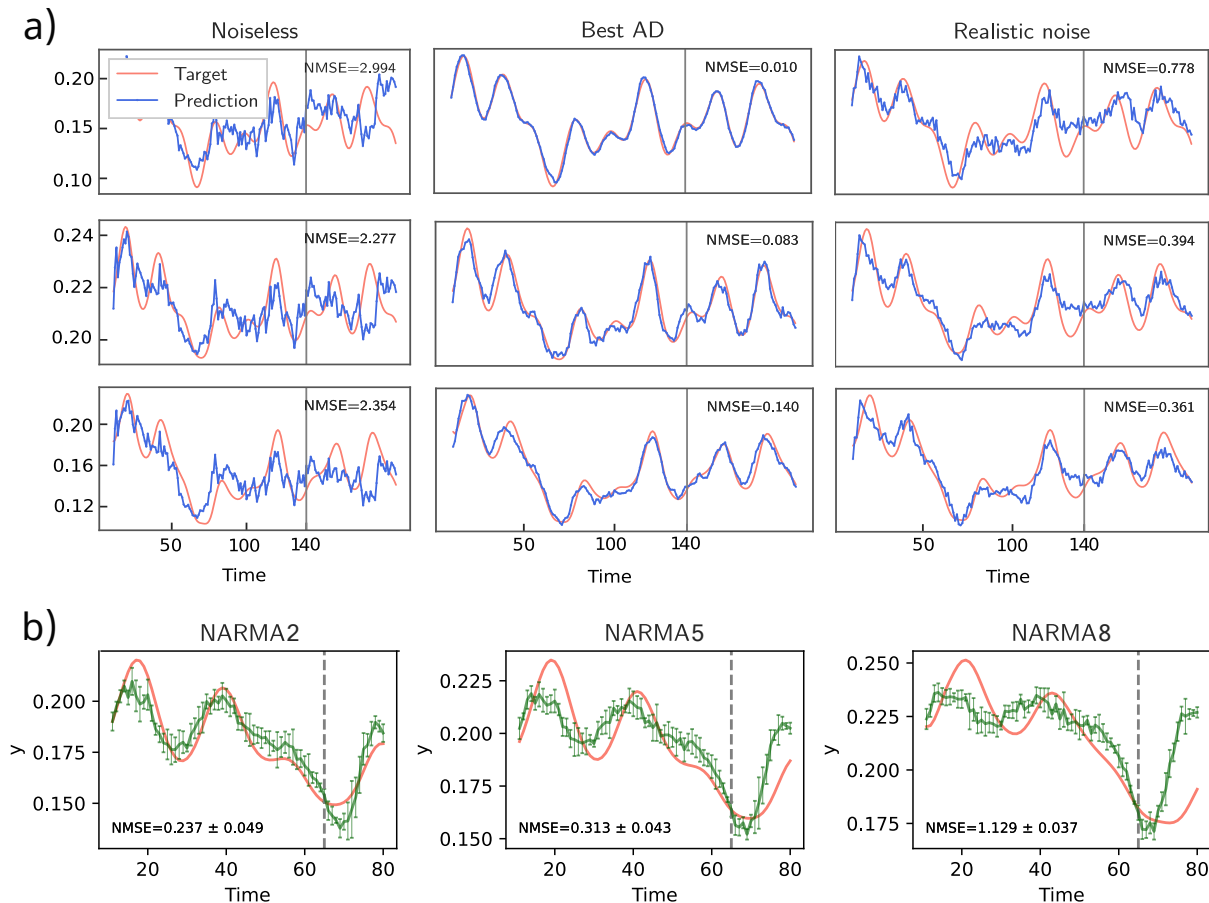


FIG. 3. **Reconstruction of NARMA tasks on simulators and quantum hardware.** a) The reconstruction of NARMA tasks for, respectively, the noiseless execution of the circuit, the execution affected by optimal amplitude damping, and the realistic noise emulating the one in IBM\_OSAKA quantum backend. Optimal values of noise are  $\gamma = 0.024, 0.03, 0.014$  for NARMA2, NARMA5 and NARMA8, respectively. The grey vertical line separates the training and test interval in the output sequence. The amplitude damping ensures the best learning of the system, which is slightly deteriorated under the composition of several noisy quantum channels representing the realistic noise. b) The experimental results of reconstruction of NARMA2, NARMA5 and NARMA8 (from left to right) tasks employing IBM\_BRISBANE quantum backend. The experiment is repeated 5 times. The mean results are reported in the green line, with error bars indicating a 1 s.d. interval. The input length is reduced, in order to reduce the depth of the circuit to fit the technical limitations of the quantum hardware. Precisely, we sample 80 values for  $u_t$ . Reconstruction deteriorates for increasing the depth in memory required, indicating the necessity of the implementation of error mitigation techniques that allow for reducing the unital noise in the evolution.

that quantum channels are non-expanding by definition [42], we may assume that the dynamics is strictly contractive since the composition of non-expanding channels and strictly contractive channels is in turn a contractive channel. Moreover, we confirmed that the realistic noise is non-unital by analyzing its effect on the Bloch sphere, as shown in Fig. 2. As expected, the network still shows a remarkable improvement in learning capabilities when compared with noiseless executions, even if the accuracy in reproducing tasks is slightly deteriorated compared to optimal pure amplitude damping. The results in the reconstruction of the NARMA task are reported in Fig. 3.

### Impact of partial and global measurements on the optimal noise regime

By tuning the intensity of pure amplitude damping in simulations, the learning capabilities of the network are maximized for  $\gamma \sim 0.02$ , corresponding to which the echo state performs best for any task. This suggests the existence of an optimal critical regime for the network's expressivity. The emergent properties of a quantum circuit depend on the rate of mid-circuit measurements performed on it [43]. This turns out to be the case also for the expressivity and the short-term memory capacity of the circuit acting as the reservoir. Indeed, when performing a complete measurement of the qubits in the register, the beneficial effect of amplitude damping appears stable

under increasing noise intensity, at least for small values of  $\lambda$  (approximately,  $\gamma < 0.1$ ). As reported in Fig. 2, this optimal value of  $\gamma$  is followed by a plateau of suboptimal values, for which the performance remains acceptable. In the case of partial measurements of the qubit register, while the optimal noise regime persists for the same noise intensity with no deterioration in memory capacity or predictive accuracy, the plateau of suboptimal values is immediately disrupted by increasing the noise intensity. Moreover, the best performances of the network essentially do not depend on the number of measured qubit.

### Experiment on superconducting quantum computer

We confirm our findings by experimenting on the IBM-Brisbane superconducting quantum computer, guided by the results of the noisy simulations. First, we employ the complete measurement of the register in order to enhance the stability under different noise intensities. As a further optimization, we introduce a tunable delay in executing rotations, deploying them as  $RZ(\alpha) = RZ(\alpha/d) \circ \dots \circ RZ(\alpha/d)$  and the same for  $RX$ , where  $\alpha$  denotes the angle of the desired rotation. Then, assuming that a delayed execution enlarges the amount of noise affecting the circuit evolution, we optimize the delay parameter  $d$  by employing the emulator, before running the experiment on quantum hardware. However, there is a trade-off to consider. Although using multiple rotations instead of a single rotation on a quantum computer helps us achieve the desired increase in error, it also comes with a downside. Quantum computers have a limited allowance for the number of operations that can be submitted, which constrains our approach. We found an optimal compromise between performances and depth of the circuit for  $d = 4$ . The experiment is conducted 5 times and the average results are shown with error bars of 1 standard deviation in Fig. 3. The experiment shows that the learning capabilities are considerably better when compared to the ideal execution without noise performed on the simulator. However, the NARMA-8 task clearly shows that when processing longer information windows is required, the unital component of the intrinsic noise in the quantum computer dominates, leading to a progressive deterioration in performance. This highlights the need to implement appropriate error mitigation techniques to eliminate the effects of unital noise or to adopt suitable strategies to amplify the impact of non-unital noise, which is undoubtedly recognized as essential in simulations.

## DISCUSSION

We showed the beneficial effect of nonunital noise in quantum reservoir computing for time-dependent tasks. In particular, we identify the noise models characterized by non-unital channels as essential for guaranteeing a drastic improvement in the learning capabilities of a quantum echo state network that employs a register of superconducting qubits as the reservoir. Indeed, we observe in numerical simulations that amplitude damping ensures great accuracy in benchmark time-dependent tasks. The learning is confirmed by conducting the experiment on the superconducting computer. Nonunitality of the evolution of the quantum circuit has already been recognized as a key resource for reservoir computing [34]. Here we show that it can be naturally induced by employing intrinsic noise in the system. Moreover, the network's response to noise qualitatively varies depending on whether complete or partial measurements are performed. In particular, in the case of complete measurements, the learning capabilities of the network remain effective over a sufficiently broad range of noise intensity values, confidently encompassing the amount of noise present in current quantum hardware. These facts pave the way for use-case results in real-world applications. Moreover, from the perspective of using quantum hardware, our results offer valuable insights that can inform best practices for developing and applying suitable error mitigation techniques. On the one hand, our observations suggest prioritizing the mitigation of dephasing and readout errors for the application of quantum reservoir computing protocols while ignoring the correction of dissipation effects. Moreover, partially effective error mitigation techniques may be employed to reduce the number of measurements since the optimal performances of the network persist in the case of partial measurement of the circuit. As a consequence, employing error control algorithms, that allow positioning within this regime, can lead to significant savings in memory consumption and execution time on quantum hardware by reducing the total number of mid-circuit measurements. Our findings are supported by the universality approximation property as proved in the Supplementary Material, which is fulfilled by our gate-based echo state network under the effect of a general set of noise quantum channels, including the amplitude damping channel.

## METHODS

### Architecture of the quantum echo state network

Our quantum echo state network exploits a  $N$ -qubits quantum register to encode and process time-dependent information and reproduce an input-output nonlinear mapping  $S(u) = \hat{y}$  between two time-dependent se-

quences  $u = \{u_t\}_{t=0,\dots,L}$  and  $\hat{y} = \{\hat{y}_t\}_{t=0,\dots,L}$ . We refer to  $u$  and  $\hat{y}$  as the input and the target sequence, respectively.

Denoting with  $\rho_t$  the density operator describing the  $N$ -qubits system at time  $t$ , its temporal evolution  $\rho_{t+1} = \mathcal{T}_{u_{t+1}}(\rho_t)$  is the composition of a noisy quantum channel, including the unitary gates that encode the input signal  $u$ , and a mid-circuit measurement operation. Precisely, at each time step, the system first evolves with the quantum evolution

$$\tilde{\rho}_{t+1} = \mathcal{E}(U(u_{t+1})\rho_t U^\dagger(u_{t+1})). \quad (5)$$

In Equation 5,  $U(u_{t+1})$  represents some unitary gates implemented by the quantum computer. Our model includes CX operators and rotations, whose angles are dependent on the incoming input value. Precisely, we encode the input value in the angle of unitary rotations as  $RX(u_t)$  and  $RZ(u_t)$ . The architecture adopted in our work is described in Fig 1.  $\mathcal{E}$  is a quantum channel that models the noise in the quantum register. Then, a mid-circuit measurement of the register is performed and the system is let evolve in the collapsed state. Formally, we have

$$\rho_{t+1} = \Pi_M \tilde{\rho}_{t+1} \Pi_M^\dagger \quad (6)$$

with, denoting with  $m_{s,t+1} \in \{0,1\}$  the outcome of the measure of the qubits  $s$  at time  $t+1$ ,

$$\Pi_M = \bigotimes_{s=1}^M |m_{s,t+1}\rangle \langle m_{s,t+1}| \otimes \mathbb{I}_{N-M} \quad (7)$$

Here,  $M$  is the number of measured qubits in the register at each time step. We remark that both the case of a complete measurement,  $M = N$ , and the case of a partial measurement,  $M < N$ , are treated in the Results. The measurement results are taken as the reservoir signal passes throughout the processing. Explicitly, the reservoir signal at time  $t$  is the expectation value of the  $\sigma_{Z(i)}$  Pauli operator of each qubit, taken separately,

$$z_t = [\langle \sigma_{Z(1)} \rangle_{\rho_t}, \dots, \langle \sigma_{Z(M)} \rangle_{\rho_t}]^T. \quad (8)$$

In our numerical experiments, the expectation value of each  $\sigma_{Z(i)}$  is obtained by repeating the experiment and computing  $\langle \sigma_{Z(i)} \rangle_{\rho_t} = \frac{1}{S} (\sum 1_{m_{i,t}=0} - \sum 1_{m_{i,t}=1})$ , where the sum is taken over all shots.

### Training of linear readout

Reservoir computing aims to reproduce best a given nonlinear map  $S(u) = \hat{y}$  by training the linear readout  $h$ . We will give examples of such learning tasks  $S(u)$  later in the work. After an initial washout period  $T_{wo}$ , required to erase the dependence on the initial state of the

network, the reservoir signal is extracted until the end of the training interval  $T_{tr}$  and it is stored in the matrix  $H = \{z_t\}_{t=T_{wo}+1,\dots,T_{tr}}$ . After the quantum evolution, the optimal readout weights are computed. Precisely, the weights of the linear readout  $y = Hw$  are chosen as the set of parameters  $w$  that minimizes the distance  $\|\hat{y} - y\|$ . It can be easily computed by linear regression or exploiting the Moore-Penrose pseudoinverse matrix, namely  $w = (H^T H)^{-1} H^T \hat{y}_{tr}$ , where  $\hat{y}_{tr} = \{\hat{y}_t\}_{t=T_{wo}+1,\dots,T_{tr}}$  is the portion of target sequence used for the training. We refer to Ref. [30] for further details on the training algorithm. After the training, the predicted values of  $y$  are given by

$$y_t = z_t \cdot w \quad \text{for any } t \in [T_{tr} + 1, L]. \quad (9)$$

It is worthwhile to notice that, thanks to the intrinsic multitasking nature of reservoir computing, the same reservoir signal can be exploited to reproduce different maps, only repeating the training to compute the optimal weights. This fact allows for the reuse of information stored in the reservoir for different tasks that share the same input, notably reducing execution time.

### Benchmark for performance analysis

Our experiments aim to demonstrate the beneficial effect of intrinsic noise in a superconducting quantum computer for reservoir computing. First, to verify whether quantum noise improves the fading memory, we study its effect on the correlation among different measurement outcomes of the same qubit over time. Then, the performances of our computational architecture under the effect of quantum noise are analyzed by exploiting standard benchmarks for recurrent neural networks. We measure the short-term memory capacity of our network using the memory capacity metric, which quantifies the amount of variance in the delayed input that can be recovered from the trained output [9]. To compute it, the system is required to replicate an input sequence  $\{u_t\}_{t=0}^T$  delayed by a time interval  $d$ . Namely, the system is required to approximate the functional  $\hat{y}_t = u_{t-d}$ . Then, the  $d$ -memory capacity is defined as

$$MC_d = \frac{\text{Cov}(y, \hat{y})}{\text{Var}(y)\text{Var}(\hat{y})}, \quad (10)$$

where  $y$  is the vector of the predicted values. The short-term memory capacity of the network is calculated as the sum up to a certain  $d_{\max}$ ,

$$MC = \frac{1}{d_{\max}} \sum_{d=1}^{d_{\max}} MC_d, \quad (11)$$

normalized so that  $MC \in [0, 1]$ . We remark that MC values closer to 1 indicate a higher memory capacity of the

system. We fix  $d_{\max} = 10$  in the numerical experiments. The predictive capabilities of our echo state network are tested with the so-called NARMA task. It is a nonlinear filter with past dependence, commonly used as a benchmark for the computational power of time-dependent learning systems [44]. Precisely, the NARMA- $p$  task is formally defined as

$$\hat{y}_t = 0.4y_t + 0.1 \left( \sum_{l=0}^{p-1} y_{t-l} \right) + u_{t-p+1} + 0.1. \quad (12)$$

We pick  $p = 2, 5$  and  $8$  in the paper. The accuracy of the prediction is quantified with the normalized mean-square error, expressed as

$$\text{NMSE}(y, \hat{y}) = \frac{\sum_{t=T_{\text{tr}}+1}^{t=L} |\hat{y}_t - y_t|^2}{\sum_{t=T_{\text{tr}}+1}^{t=L} \hat{y}_t^2} \quad (13)$$

where  $y$  is the vector of the predicted values after training. The input time series  $u_t$  is sampled from the continuous function  $f(t) = 0.1 \sin\left(\frac{2\pi\alpha t}{T}\right) \cdot \sin\left(\frac{2\pi\beta t}{T}\right) \cdot \sin\left(\frac{2\pi\delta t}{T}\right)$  with  $(\alpha, \beta, \delta, T) = (2.11, 3.73, 4.11, 200)$ .

### Ideal and realistic quantum noise models

The effect of noise in a quantum computer can be simulated by repeatedly applying a quantum channel to the density operator that describes the state of the qubit register. Precisely, in numerical simulations, a quantum channel  $\mathcal{E}$ , representing a certain noise model, is applied to each qubit after the action of each unitary gate  $U$ , as shown in Equation 5. First, we investigate the effect of three typical ideal models of quantum noise. Namely, we test the effect of amplitude damping, phase damping, and depolarizing noises. We recall that a quantum channel can always be expressed in terms of its Kraus decomposition,

$$\mathcal{E}(\rho) = \sum_{i=1}^r K_i \rho K_i^\dagger. \quad (14)$$

We refer to Table 1 in the Supplementary Material for a detailed description of the Kraus operators of the three noise models considered in this work. The noise intensity is tuned by a parameter appearing in the Kraus decomposition, which we indicate with  $\gamma$  throughout the paper. Smaller  $\gamma$  values correspond to a final quantum state less affected by noise. After the preliminary analysis of the effect of an ideal pure noise, we test our architecture with a more realistic model of quantum noise, which faithfully emulates noise in a superconducting device. To do this, we apply the quantum channels that model the noise of IBMQ backends freely available to the user. The simulation of a backend noise model implemented by Qiskit [45] exploits a combination of thermal relaxation and depolarizing channels.

### Experimental settings

In this work, we fix  $N = 7$  as the number of qubits. In numerical simulations, we consider a total timespan of  $L = 200$ , with a washout period of 10 time steps ( $T_{\text{wo}} = 10$ ), while the test interval is 60 time steps long. Each circuit is run for  $S = 10^5$  shots for a precise reconstruction of the average value of observables. All the simulations with an ideal noise model are run over 100 different values of  $\gamma$ . Preliminary experiments are conducted using the Qiskit simulator [45]. In experiments involving the quantum hardware, we significantly reduce the depth of the circuit due to technical limitations of the cloud service employing the IBM quantum service and cost management. In particular, we fix  $L = 80$ , and for each experiment, we submit 90 jobs in batch, with 5 circuits each and 30 shots per shot, for a total of 13500 shots. We used the IBM\_BRISBANE quantum processing unit, which mounts an Eagle processor, equipped with 127 qubits. For the simulations, we used a 36-core Intel Xeon processor (4.3 GHz) with 128 GB of RAM.

### ACKNOWLEDGEMENTS

F.M. and E.P. are supported by PRIN-PNRR Physi-Comp (nr. grant G53D23006710001). L.N. is partially funded by ENI S.p.A.

### CODE AVAILABILITY

The code is made available by the authors upon reasonable request.

### COMPETING INTERESTS

Authors declares no competing interests.



*Supplementary material to: "Non-unital noise as a computational resource for quantum reservoir computing"*

## QUANTUM RESERVOIR COMPUTING AND FADING MEMORY

Denoting  $\mathcal{S}(\mathcal{H})$  the set of density operators on the Hilbert space  $\mathcal{H}$  that describes some quantum system, we recall that is possible to describe a quantum reservoir computer with the equations

$$\begin{cases} \rho_{t+1} = \mathcal{T}(\rho_t, u_{t+1}) \\ y_{t+1} = h(\rho_{t+1}) \end{cases} \quad (15)$$

where  $\mathcal{I} \ni u = \{\dots, u_{-1}, u_0\}$  is the input signal and  $\mathcal{T} : \mathcal{S}(\mathcal{H}) \rightarrow \mathcal{S}(\mathcal{H})$  is a quantum channel that describes the dynamic of the reservoir. The key property of a reservoir computer is the well-known echo state property (or, convergence property) [41], which ensures that for each input sequence  $u$ , there exists a unique reservoir signal  $z$ . If the echo state property holds, the reservoir computer defines a unique, causal operator  $\mathcal{C} : \mathcal{I} \rightarrow \mathcal{O}$  defined by

$$\mathcal{C}(u)_t = \mathcal{C}(u|_t) = h(\mathcal{T}(\rho_{t-1}, u_t)) \quad (16)$$

where  $u|_t$  is the sequence  $u$  truncated at time  $t$ . As a consequence, it defines a unique functional on the set of input sequences as  $C(u) = \mathcal{C}(u)_0$ . Note that the choice of  $t = 0$  as the final time step is merely irrelevant since the system is time-invariant. Fading memory is formally defined as the continuity of this functional, and thus of related filter since the relation is bijective, with respect to a proper topology.

**Definition .1** (Fading memory). *Let  $\omega : \mathbb{Z}^- \rightarrow (0, 1]$  be an increasing function with zero limit at infinity and  $\omega(0) = 1$  and define the distance*

$$d_\omega(u, v) = \sup_{t \in \mathbb{Z}^-} \|u_t - v_t\| \omega_t, \quad \forall u, v \in \mathcal{I}. \quad (17)$$

*A reservoir computer has fading memory if the associated functional  $\mathcal{C} : \mathcal{I} \rightarrow \mathbb{R}$  is continuous in the topology of the metric space  $(\mathcal{I}, d_\omega)$ .*

Fading memory of a quantum reservoir ultimately depends on the properties of the quantum channel  $\mathcal{T}$  that defines the quantum reservoir computer. In particular, there is the following important theorem, that ensures fading memory.

**Theorem .2** (Theorem 3 in [39]). *If the quantum channel  $\mathcal{T}$  is strictly contractive in the trace norm  $\|A\|_1 = \text{tr}(\sqrt{A^\dagger A})$ , namely*

$$\|\mathcal{T}(\rho) - \mathcal{T}(\sigma)\|_1 \leq r \|\rho - \sigma\|_1 \quad (18)$$

*for some  $r \in (0, 1)$ , then the associated reservoir computer has the echo state property and fading memory.*

We remark that any quantum channel is non-expansive in trace norm, namely

$$\|\mathcal{T}(\rho)\|_1 \leq \|\rho\|_1. \quad (19)$$

## A GEOMETRICAL INTERPRETATION OF NON-UNITAL CHANNELS

Quantum channels that preserve identity, namely  $\mathcal{T}(\mathbb{I}) = \mathbb{I}$ , are said to be unital. Unital channels are not suitable for reservoir computing, as shown by the following theorem. Here  $\mathcal{B}(\mathcal{H})$  is the set of all bounded operators and  $d$  is the dimension of the Hilbert space.

**Theorem .3** (Theorem 5 in [42]). *Assume there exists  $\epsilon > 0$  and an operator norm  $\|\cdot\|$  such that the channel  $\mathcal{T}(\cdot, u) : \mathcal{B}(\mathcal{H}) \rightarrow \mathcal{B}(\mathcal{H})$  satisfies  $\|\mathcal{T}(\cdot, u)\| \leq 1 - \epsilon$  for any  $u \in \mathcal{I}$ . Then, the correspondent functional  $\mathcal{C}$  defined the reservoir computer in Eq.15 is constant with  $\mathcal{C}(u) = h(\mathbb{I}/d)$  if and only if  $\mathcal{T}$  is unital for any input, namely  $\mathcal{T}(\mathbb{I}, u) = \mathbb{I} \quad \forall u \in \mathcal{I}$ .*

The action of unital channels has a geometrical interpretation in the Bloch sphere representation of qubit state, which allows distinguishing between unitality and non-unitality of a given channel, even without knowing its analytical expression. The set of pure states in the image of a quantum channel  $\mathcal{E}$  is called its pure output PO( $\mathcal{E}$ ), namely

$$\text{PO}(\mathcal{E}) = \{\mathcal{E}(\rho), \forall \rho \in \mathcal{S}(\mathcal{H})\} \cap \mathcal{P}. \quad (20)$$

In the Bloch sphere, the pure output is the intersection between the spherical surface of the pure states and the ellipsoid representing the image of the quantum channel. Unital channels fulfill a fundamental symmetry property.

**Theorem .4** (Lemma 4.3 in [46]). *The pure output of an unital channel  $\mathcal{T}$  is centrally symmetric.*

Hence, by looking at the pure output of a quantum channel we are able to determine whether it is unital or not [46]. In particular, the channel is unital if and only if the center of the image ellipsoid coincides with the center of the Bloch sphere. This fact has a trivial interpretation since the center of the Bloch sphere corresponds to the maximally mixed state  $\rho = \mathbb{I}/2$ . Precisely, we recall the following theorem.

**Theorem .5** (Theorem 4.9 in [46]). *Let  $\mathcal{E}$  be a qubit channel and  $\mathcal{P}$  the set of pure states. One of the following holds:*

1.  $\text{PO}(\mathcal{E}) = \emptyset$ , the channel has no pure output;
2.  $\text{PO}(\mathcal{E}) = \{\xi\}$ , the channel has a unique pure output state  $\xi$ ;
3.  $\text{PO}(\mathcal{E}) = \{\xi, \zeta\}$ , the channel has exactly two pure outputs  $\xi, \zeta$ ;

Noise model	Description	Kraus decomposition
Amplitude damping	Loss of energy to the environment	$K_0 = \begin{pmatrix} 1 & 0 \\ 0 & \sqrt{1-\gamma} \end{pmatrix}, K_1 = \begin{pmatrix} 0 & \sqrt{\gamma} \\ 0 & 0 \end{pmatrix}$
Phase damping	Loss of quantum information	$K_0 = \sqrt{1-\gamma}\mathbb{I}, K_1 = \begin{pmatrix} \sqrt{\gamma} & 0 \\ 0 & 0 \end{pmatrix}, K_2 = \begin{pmatrix} 0 & 0 \\ 0 & \sqrt{\gamma} \end{pmatrix}$
Depolarizing	Decay to maximally mixed state	$K_0 = \sqrt{1-\gamma}\mathbb{I}, K_1 = \sqrt{\gamma}X, K_2 = \sqrt{\gamma}Y, K_3 = \sqrt{\gamma}Z$

TABLE I. The Kraus decomposition of the quantum channel describing respectively amplitude damping, phase damping, and depolarizing noise.

#### 4. $\text{PO}(\mathcal{E}) = \mathcal{P}$ , all pure states are in the image of $\mathcal{E}$ .

In particular, combining Theorem 4 and Theorem 5, we can deduce that a channel with exactly two pure outputs is unital if and only if they are antipodal on the Bloch sphere (thus, are orthogonal in the Hilbert space). Fig. 5 in the Main text shows the action of amplitude damping, depolarizing, phase damping, and fake-OSAKA channel. As expected, amplitude damping is the sole non-unital ideal noise channel. Moreover, we can observe that the fake-OSAKA channel is non-unital.

### CONTRACTIVITY OF NOISE CHANNELS

In this Appendix, we prove that a noise channel  $\mathcal{D} : \mathcal{S}(\mathcal{H}) \rightarrow \mathcal{S}(\mathcal{H})$  ensures fading memory by proving that it is strictly convergent in the trace norm. Namely, we show that there exists  $r < 1$  such that  $\|D(\rho) - D(\sigma)\|_1 \leq r\|\rho - \sigma\|_1$ . For clarity, we write the proof for the single-qubit Hilbert space  $\mathcal{H} = \mathbb{C}^2$ . The extension to the multidimensional case is trivial. Now we propose some common noise channels and evaluate whether they guarantee fading memory or not. In order to do so, it is helpful to Kraus decompose each channel [47], hence write each channel in the form

$$\mathcal{D}(\rho) = \sum_i K_i \rho K_i^\dagger. \quad (21)$$

For the following calculations, it is useful to keep in mind that for a generic Kraus operator  $K$  we have

$$\begin{aligned} \|K \rho K^\dagger\|_1 &= K_{ij} \rho_{jl} K_{li}^\dagger = k_i \delta_{ij} \rho_{jl} k_l \delta_{li} = \\ &= k_i \rho_{ii} k_i = k_i^2 \rho_{ii} \end{aligned} \quad (22)$$

where summation is implied over repeated indices. Remarkably the set of strictly contractive quantum channels is dense in the set of all quantum channels [48]. That is, in the assumption of finite resolution in the observations, we can assume that any channel modeling noise is strictly contractive, thus ensuring fading memory to the system.

**Bit flip, bit-phase flip and phase flip.** The Kraus decomposition of the bit flip map is

$$\mathcal{D}_{\text{bf}}(\rho) = \sqrt{1-\gamma}\rho + \sqrt{\gamma}X\rho X. \quad (23)$$

Notice that the bit-phase flip and the phase flip maps have the same form of the bit flip, but instead of the  $X$  Pauli operator, they involve the  $Y$  and  $Z$  operators, respectively. Hence we have

$$\mathcal{D}_{\text{bpf}}(\rho) = \sqrt{1-\gamma}\rho + \sqrt{\gamma}Y\rho Y. \quad (24)$$

$$\mathcal{D}_{\text{pf}}(\rho) = \sqrt{1-\gamma}\rho + \sqrt{\gamma}Z\rho Z. \quad (25)$$

Then, for the sake of conciseness, we only show the case of the bit flip, the other cases being a trivial extension. Since Pauli operators are traceless operators, we can identify

$$K_0 = \sqrt{1-\gamma}\mathbb{I} \quad \text{and} \quad K_1 = \sqrt{\gamma}X \quad (26)$$

By exploiting Equation 22, we have trivially

$$\|K_0(\rho - \sigma)K_0^\dagger\|_1 \leq 2(1-\gamma)|\rho_{00} - \sigma_{00}| \quad (27)$$

and

$$\|K_1(\rho - \sigma)K_1^\dagger\|_1 = 0. \quad (28)$$

Thus, such channels are contractive in trace norm.

**Amplitude damping.** The quantum operation that describes energy dissipation is the amplitude damping quantum channel. Recalling the Kraus decomposition of the amplitude damping channel, we have

$$\mathcal{D}_{\text{ad}}(\rho) = K_0 \rho K_0^\dagger + K_1 \rho K_1^\dagger \quad (29)$$

with  $K_0 = \begin{pmatrix} 1 & 0 \\ 0 & \sqrt{1-\gamma} \end{pmatrix}$  and  $K_1 = \begin{pmatrix} 0 & \sqrt{\gamma} \\ 0 & 0 \end{pmatrix}$ . We consider the two terms separately, exploiting Equation 22. Thus, since  $\text{tr}(\rho) = \text{tr}(\sigma) = 1$ , for the first Kraus operator we conclude that

$$\|K_0(\rho - \sigma)K_0^\dagger\|_1 = |\rho_{00} - \sigma_{00}| (1 + \sqrt{1-\gamma}) \leq \quad (30)$$

$$\leq r\|\rho - \sigma\|_1 = 2|\rho_{00} - \sigma_{00}| \quad (31)$$

with  $r = 1 - \frac{\gamma}{2} < 1$ . Similarly, for the other term, we get

$$\|K_1(\rho - \sigma)K_1^\dagger\|_1 \leq r\|\rho - \sigma\|_1 \quad (32)$$

for  $r = \gamma/2$ . We conclude that  $D$  is strictly contractive, since

$$\|\mathcal{D}_{\text{ad}}(\rho) - \mathcal{D}_{\text{ad}}(\sigma)\|_1 \leq \|K_0(\rho - \sigma)K_0^\dagger\|_1 + \quad (33)$$

$$+ \|K_1(\rho - \sigma)K_1^\dagger\|_1 \leq r\|\rho - \sigma\|_1 \quad (34)$$

with  $r = \max(1 - \frac{\gamma}{2}, \gamma/2) < 1$ .

**Depolarizing channel.** Consider a qubit that has probability  $p$  of being depolarized. The action of the depolarizing channel is represented by

$$\mathcal{D}_{\text{de}}(\rho) = \frac{p}{2}\mathbb{I} + (1-p)\rho. \quad (35)$$

In the operator-sum representation, we can write

$$\left(1 - \frac{3p}{4}\right)\rho + \frac{p}{4}(X\rho X + Y\rho Y + Z\rho Z) \quad (36)$$

or, equivalently, it is more commonly written as

$$(1-p)\rho + \frac{p}{3}(X\rho X + Y\rho Y + Z\rho Z) \quad (37)$$

which means that the state  $\rho$  is left alone with probability  $1-p$ , and each Pauli operator acts with probability  $p/3$ .

**Phase damping.** The loss of information, without loss of energy, is described by the phase damping. We observe that the phase damping channel can be written as

$$\mathcal{D}_{\text{pd}}(\rho) = \tilde{K}_0\rho\tilde{K}_0 + \tilde{K}_1\rho\tilde{K}_1 \quad (38)$$

with

$$\tilde{K}_0 = \begin{pmatrix} 1 & 0 \\ 0 & \sqrt{1-\lambda} \end{pmatrix} \quad (39)$$

$$\tilde{K}_1 = \begin{pmatrix} 0 & 0 \\ 0 & \sqrt{\lambda} \end{pmatrix}$$

where the parameter  $\lambda$  can be interpreted as the probability of having a photon scattered (without loss of energy) as it travels through a waveguide.

An important thing to notice is that by a unitary recombination of  $\tilde{K}_0$  and  $\tilde{K}_1$ , we can write other two equivalent Kraus operators for the phase damping channel: define  $\gamma = (1 - \sqrt{1-\lambda})/2$ , then

$$\begin{pmatrix} K_0 = \sqrt{1-\gamma}\mathbb{I} \\ K_1 = \sqrt{\gamma}X \end{pmatrix}. \quad (40)$$

Thus, phase damping describes the same operation as the phase flip. Hence it inherits the same contraction and unitality properties.

**Thermal relaxation.** Thermal relaxation is equivalent to phase-amplitude damping. The problem is that the Qiskit implementation of the thermal relaxation

channel differs from the standard one, hence a short comment is needed. Thermal relaxation, in the Qiskit version, is modeled by the following Kraus decomposition in Qiskit [45]:

$$\begin{aligned} K_0 &= \sqrt{1-p_z-p_{r0}-p_{r1}}\mathbb{I} \\ K_1 &= \sqrt{p_z}Z \\ K_2 &= \sqrt{p_{r0}}\begin{pmatrix} 1 & 0 \\ 0 & 0 \end{pmatrix} \\ K_3 &= \sqrt{p_{r1}}\begin{pmatrix} 0 & 0 \\ 0 & 1 \end{pmatrix} \end{aligned} \quad (41)$$

where  $p_z$  is the probability of phase flip,  $p_{r0}$  is the reset probability to state  $|0\rangle\langle 0|$  and  $p_{r1}$  is the reset probability to state  $|1\rangle\langle 1|$ .

## UNIVERSAL APPROXIMATION PROPERTY OF OUR GATE-BASED ECHO STATE NETWORK

A family of computational architectures is universal for a certain set of functionals if, for any of these mappings, there exists an instance within the family that approximates it with arbitrary precision [38]. In particular, the universality of a family of reservoir computers for fading memory mappings relies on some general sufficient conditions [10] – generalized by some of the Authors to comprehensively include quantum reservoir computing regardless of any specific implementation [40]. Here, we prove that the gate-based quantum echo state network is universal under the action of nonunital and strictly contractive noise models, thus providing theoretical support to our findings. We begin by recalling the sufficient conditions that ensure the universality, summarized in the following theorem [40].

**Theorem .6.** *Let  $\mathcal{R}$  be a family of real echo reservoir computers and let  $\mathcal{I} = \{u: \mathbb{Z} \rightarrow [0, 1]\}$  be the set of input sequences. Assume that  $(\mathcal{I}, d_\omega)$  is a compact metric space. If the set of functionals  $\mathcal{H}_{\mathcal{R}}$  associated with  $\mathcal{R}$ :*

- *has fading memory*
- *separates points in  $\mathcal{I}$ , namely for any pair  $u, v \in \mathcal{I}$  with  $u \neq v$  there exists a functional  $H \in \mathcal{H}_{\mathcal{R}}$  such that  $Hu \neq Hv$ ;*
- *is polynomial algebra, namely for any  $R_1, R_2 \in \mathcal{H}_{\mathcal{R}}$  there exist  $R_+^\lambda, R_\times \in \mathcal{H}_{\mathcal{R}}$  such that  $R_1(u) + \lambda R_2(u) = R_+^\lambda(u)$  and  $R_1(u) \cdot R_2(u) = R_\times(u)$  for any  $u \in \mathcal{I}$ ;*

*then  $\mathcal{R}$  is universal for the set of mappings with fading memory.*

### Compactness of the input space

The mathematical proof of universality relies on the Stone-Weierstrass theorem, which applies to compact metric space. Thus, to ensure universality, we have to check that the input space, equipped with the fading metric introduced above is a compact metric space. This is a general result for time series inputs and it follows from the following theorem, proved also in [40].

**Lemma .7.** *The space of bounded time-dependent sequences  $\mathcal{I}$  equipped with the distance  $d_\omega$  defined in Def. .1 is a compact metric space.*

### Echo state property and fading memory of the associated functional

A reservoir computer fulfills echo state property if the internal dynamics of the network does not depend explicitly on its specific initialization. This implies that the reservoir computer defines a unique, well-posed mapping between  $\mathcal{I}$  and  $\mathcal{O}$ . As discussed above, both the echo state property and the fading memory follow if the dynamics is strictly contractive in the trace norm. Thus, these properties follow from the strict contractivity of the quantum channel that models the evolution of the echo state network, namely,

$$\tilde{\rho}_{t+1} = \mathcal{E}(U(u_{t+1})\rho_t U^\dagger(u_{t+1}))$$

since the measurement process does not erase the strict contractivity of the overall evolution.

### Separability of the inputs

A universal class of reservoir computers has the ability to discriminate any pair of different inputs. Namely, for any given  $u, v \in \mathcal{I}$ , the dynamics of a reservoir in the class should be such that associated mapping has different outputs when evaluated on  $u$  and  $v$ , respectively. We proceed by constructing it, exploiting a single qubit reservoir and the action of suitable quantum channels. Denoting with  $x \in [0, 1]$  the current value of the input, the dynamics of reservoir register is written as

$$\rho_{t+1} = \Phi_x(\rho_t) = \mathcal{E}(U(x)\rho_t U^\dagger(x)). \quad (42)$$

Then, we can prove the following Theorem that ensures the separability of the input under suitable conditions on the dynamics.

**Theorem .8.** *If the dynamics described by Eq. (42) has a unique fixed point  $\rho_*^x$ , that depends univocally on  $x$ , then we have separability.*

In fact, without loss of generality, let assume  $u, v \in \mathcal{I}$  such that  $u_t = v_t \forall t \neq 0$  and  $u_0 = v_0$ , and let denote with  $\rho_t^y$ ,  $y = u, v$  the state of the circuit after the injection of  $u$  and  $v$ , respectively. Since the input sequences are equal for  $t < 0$ , we assume moreover that  $\rho_0^u = \rho_0^v$ . Preparing the circuit in the fixed point  $\rho_*^{u_0}$ , immediately we realize that  $\rho_1^u \neq \rho_1^v$  since the fixed point  $\rho_1^u = \rho_*^{u_0}$  depends univocally on  $u_0$ . Then the dynamics continues separated, as indeed the linear operator  $e^{\mathcal{L}t(y)}$ , that encodes the evolution in Eq. (42), is a linear full rank operator.

It remains to show that there exists a quantum channel  $\mathcal{E}$  such that Eq. (42) has a unique fixed point. This is the case for the amplitude damping channel.

**Lemma .9.** *If the quantum channel in Eq. (42) is the amplitude damping  $\mathcal{E}_{ad}$ , then the equation has a unique fixed point that depends univocally on the value of the input.*

*Proof.* It suffices to recall that the unique fixed point of the amplitude damping channel is the  $|0\rangle$  state, namely  $\mathcal{E}_{ad}(\rho) = \rho$  if and only if  $\rho = |0\rangle\langle 0|$ . Then, the fixed point of the composed map  $\rho_{t+1} = \mathcal{E}_{ad}(U(x)\rho_t U^\dagger(x))$  is simply  $\rho_*^x = U^\dagger(x)|0\rangle\langle 0|U(x)$ , which depends univocally on  $x$ .  $\square$

We remark that, on the other hand, if the quantum channel  $\mathcal{E}$  is unital, namely if it preserves the identity density operator  $\mathcal{E}(\mathbb{I}) = \mathbb{I}$ , the dynamics has a fixed point that does not depend on the input values. Indeed, by definition of the unitality of a quantum channel, we have that

$$\Phi_x(\rho_*) = \rho_* \iff \rho_* = U(x)\mathbb{I}U^\dagger(x) = U(x)U^\dagger(x)\mathbb{I} = \mathbb{I}.$$

regardless of the value of the input  $x$ .

### Polynomial algebra structure by spatial multiplexing

It remains to prove that the associated mappings form a polynomial algebra, to ensure the universality of our family of quantum echo state networks. This can be achieved by exploiting spatial multiplexing, as widely known in the context of quantum reservoir computing [18, 27, 29]. It consists of parallelly preparing and running the two networks and taking the sum, or the product, of the readouts as the overall readout function. Then, for any two echo state networks whose associated mapping are respectively  $\mathcal{C}_1$  and  $\mathcal{C}_2$ , it is possible to construct the systems whose associated mapping is the sum  $\mathcal{C}_1 + \mathcal{C}_2$  and the product  $\mathcal{C}_1 \cdot \mathcal{C}_2$ . Adding this multiplexed architecture to the general class, we recover the structure of the polynomial algebra of the mappings associated. Thus, combining the previous Subsections, we have proved that, under suitable conditions on the quantum

channel - for example, fulfilled by the amplitude damping channel - our class of gate-based echo state networks described is universal for the class of filters with fading memory.

---

\* enrico.prati@unimi.it

- [1] Deutsch, I. H. Harnessing the power of the second quantum revolution. *PRX Quantum* **1**, 020101 (2020).
- [2] Prati, E. Quantum neuromorphic hardware for quantum artificial intelligence. In *Journal of Physics: Conference Series*, vol. 880 (IOP Publishing, 2017).
- [3] Biamonte, J. *et al.* Quantum machine learning. *Nature* **549**, 195–202 (2017).
- [4] Verstraete, F., Wolf, M. M. & Cirac, J. I. Quantum computation and quantum-state engineering driven by dissipation. *Nature Physics* **5** (2009).
- [5] Rocutto, L. & Prati, E. A complete restricted boltzmann machine on an adiabatic quantum computer. *International Journal of Quantum Information* **19**, 2141003 (2021).
- [6] Noè, D., Rocutto, L., Moro, L. & Prati, E. Quantum parallel training of a boltzmann machine on an adiabatic quantum computer. *Advanced Quantum Technologies* 2300330 (2024).
- [7] Fefferman, B., Ghosh, S., Gullans, M., Kuroiwa, K. & Sharma, K. Effect of nonunitary noise on random-circuit sampling. *PRX Quantum* **5** (2024).
- [8] Mele, A. A. *et al.* Noise-induced shallow circuits and absence of barren plateaus (2024). 2403.13927.
- [9] Jaeger, H. Short term memory in echo state networks (2001).
- [10] Maass, W. W., Natschläger, T. & Markram, H. Real-time computing without stable states: a new framework for neural computation based on perturbations. *Neural Computation* (2002).
- [11] Nakajima, K. & Fischer, I. *Reservoir Computing. Theory, Physical Implementations, and Applications* (Springer Singapore, 2021).
- [12] Tanaka, G. *et al.* Recent advances in physical reservoir computing: a review. *Neural Networks* **115** (2019).
- [13] Marković, D. & Grollier, J. Quantum neuromorphic computing. *Applied Physics Letters* **117** (2020).
- [14] Mujal, P. *et al.* Opportunities in quantum reservoir computing and extreme learning machines. *Advanced Quantum Technologies* **4** (2021).
- [15] Spagnolo, M., Morris, J., Piacentini, S. *et al.* Experimental photonic quantum memristor. *Nature Photonics* **16**, 318–323 (2022).
- [16] Nakajima, M., Tanaka, K. & Hashimoto, T. Scalable reservoir computing on coherent linear photonic processor. *Communications Physics* **4** (2021).
- [17] García-Beni, J., Giorgi, G. L., Soriano, M. C. & Zambrini, R. Scalable photonic platform for real-time quantum reservoir computing. *Phys. Rev. Appl.* **20** (2023).
- [18] Nokkala, J. *et al.* Gaussian states of continuous-variable quantum systems provide universal and versatile reservoir computing. *Communications Physics* **4** (2021).
- [19] Govia, L. C. G., Ribeill, G. J., Rowlands, G. E., Krovi, H. K. & Ohki, T. A. Quantum reservoir computing with a single nonlinear oscillator. *Phys. Rev. Res.* **3**, 013077 (2021).
- [20] Ghosh, S., Krisnanda, T., Paterek, T. & Liew, T. C. H. Realising and compressing quantum circuits with quantum reservoir computing. *Communications Physics* **4** (2021).
- [21] Ghosh, S., Opala, A., Matuszewski, M., Paterek, T. & Liew, T. C. H. Quantum reservoir processing. *npj Quantum Information* **5** (2019).
- [22] Bravo, R. A., Najafi, K., Gao, X. & Yelin, S. F. Quantum reservoir computing using arrays of rydberg atoms. *PRX Quantum* **3**, 030325 (2022).
- [23] Fujii, K. & Nakajima, K. Harnessing disordered-ensemble quantum dynamics for machine learning. *Phys. Rev. Appl.* **8** (2017).
- [24] Nakajima, K., Fujii, K., Negoro, M., Mitarai, K. & Kitagawa, M. Boosting computational power through spatial multiplexing in quantum reservoir computing. *Phys. Rev. Appl.* **11** (2019).
- [25] Chen, J. & Nurdin, H. I. Learning nonlinear input–output maps with dissipative quantum systems. *Quantum Information Processing* **18** (2019).
- [26] Pablo Mujal, G. L. G., Raúl Martínez-Peña *et al.* Time-series quantum reservoir computing with weak and projective measurements. *npj Quantum Information* **9** (2023).
- [27] Sannia, A., Martínez-Peña, R., Soriano, M. C., Giorgi, G. L. & Zambrini, R. Dissipation as a resource for Quantum Reservoir Computing. *Quantum* **8**, 1291 (2024).
- [28] De Michielis, M. *et al.* Silicon spin qubits from laboratory to industry. *Journal of Physics D: Applied Physics* **56**, 363001 (2023).
- [29] Chen, J., Nurdin, H. I. & Yamamoto, N. Temporal information processing on noisy quantum computers. *Phys. Rev. Appl.* **14** (2020).
- [30] Molteni, R., Destri, C. & Prati, E. Optimization of the memory reset rate of a quantum echo-state network for time sequential tasks. *Phys. Lett. A* (2023).
- [31] Kubota, T. *et al.* Temporal information processing induced by quantum noise. *Physical Review Research* **5**, 023057 (2023).
- [32] Maass, W. & Markram, H. On the computational power of circuits of spiking neurons. *J. Comput. Syst. Sci.* (2004).
- [33] Monzani, F. & Prati, E. Universality conditions of unified classical and quantum reservoir computing (2024). 2401.15067.
- [34] Hu, F. *et al.* Overcoming the coherence time barrier in quantum machine learning on temporal data. *Nature communications* **15**, 7491 (2024).
- [35] Domingo, L., Carlo, G. & Borondo, F. Taking advantage of noise in quantum reservoir computing. *Sci. Rep.* (2023).
- [36] Bertschinger, N., Natschläger, T. & Legenstein, R. At the edge of chaos: Real-time computations and self-organized criticality in recurrent neural networks. In *Advances in Neural Information Processing Systems* (2004).
- [37] Martínez-Peña, R., Giorgi, G. L., Nokkala, J., Soriano, M. C. & Zambrini, R. Dynamical phase transitions in quantum reservoir computing. *Phys. Rev. Lett.* (2021).
- [38] Hornik, K., Stinchcombe, M. & White, H. Multilayer feedforward networks are universal approximators. *Neural Networks* **2**, 359–366 (1989).

- [39] Grigoryeva, L. & Ortega, J.-P. Echo state networks are universal. *Neural Networks* **108** (2018).
- [40] Monzani, F. & Prati, E. Universality conditions of unified classical and quantum reservoir computing. arXiv: 2401.15067 (2024).
- [41] Jaeger, H. The” echo state” approach to analysing and training recurrent neural networks-with an erratum note’. *Bonn, Germany: German National Research Center for Information Technology GMD Technical Report* **148** (2001).
- [42] Martínez-Peña, R. & Ortega, J.-P. Quantum reservoir computing in finite dimensions. *Physical Review E* **107** (2022).
- [43] Koh, J. M., Sun, S.-N., Motta, M. & Minnich, A. J. Measurement-induced entanglement phase transition on a superconducting quantum processor with mid-circuit readout. *Nat. Phys.* (2023).
- [44] Atiya, A. & Parlos, A. New results on recurrent network training: unifying the algorithms and accelerating convergence. *IEEE Transactions on Neural Networks* **11** (2000).
- [45] Qiskit contributors. Qiskit: An open-source framework for quantum computing (2023).
- [46] Braun, D., Giraud, O., Nechita, I., Pellegrini, C. & Žnidarič, M. A universal set of qubit quantum channels. *Journal of Physics A: Mathematical and Theoretical* **47**, 135302 (2014).
- [47] Nielsen, M. A. & Chuang, I. L. *Quantum Computation and Quantum Information* (Cambridge University Press, 2010).
- [48] Raginsky, M. Strictly contractive quantum channels and physically realizable quantum computers. *Physical Review A* **65** (2001).